JACS
JOURNAL OF THE AMERICAN CHEMICAL SOCIETY

ARTICLE

pubs.acs.org/JACS

Interaction of a Weakly Acidic Dinitroaromatic with Alkylamines: Avoiding the Meisenheimer Trap

Eric J. Olson, Teng T. Xiong, Christopher J. Cramer, and Philippe Bühlmann*

Department of Chemistry and Supercomputing Institute, University of Minnesota, 207 Pleasant Street SE, Minneapolis, Minnesota 55455, United States

Supporting Information

ABSTRACT: Polynitroaromatics are well-known to form anionic σ-complexes (Meisenheimer complexes). The formation of such complexes was assumed in the past to explain the blue color of solutions of 2,4-dinitrotoluene (DNT) and amines. However, this work shows that caution is warranted to avoid the hasty misidentification of Meisenheimer complexes. ^{1}H NMR spectra exhibit no significant shifts in the positions of the DNT protons, indicating that the majority of DNT species in solutions of DNT and amines retain their aromaticity. Density functional calculations on DNT−ethylamine complexes suggest that Meisenheimer complexes are sufficiently high in free energy so that they make up only a very small fraction of the full equilibrium population. While principal component analysis of the UV/vis spectra of the DNT−amine solutions reveals that only one absorbing species of significant concentration is formed, quantitative fits of Job's plots show that 1:1 association of DNT with the amines alone cannot explain the visible absorption spectra. Instead, the Job's plots can be accurately interpreted by deprotonation of DNT, with the amines acting as bases. The deprotonation equilibria lie far on the side of the unreacted DNT, preventing the detection by NMR of the deprotonated minority species that gives the solutions their strong blue color. The analysis of systems with DNT and *n*-butylamine, diethylamine, triethylamine, or benzylamine provides a consistent pK_a of DNT in dimethyl sulfoxide of 15.3 ± 0.2.

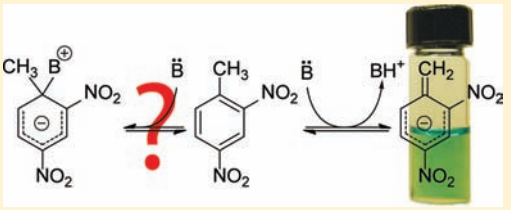

1. INTRODUCTION

The analysis of 2,4-dinitrotoluene (DNT) is of interest because of its role as an intermediate in the synthesis of polyurethane and its hepatocarcinogenicity.[1] However, the key incentive for developing chemical sensors for DNT lies in the detection of explosives[2−4] since DNT is a common impurity in the widely used explosive 2,4,6-trinitrotoluene (TNT).[5] While various sensing schemes for the detection of TNT itself have been reported, including several ones based on the formation of colored complexes,[6−9] the detection of its impurity DNT is often preferable for analytical purposes as its much higher volatility allows a much more sensitive detection. Indeed, dogs trained to find TNT smell primarily DNT and not TNT.[5] Not surprisingly, chemical abstracts lists nearly 4000 entries for DNT.

For the design of DNT receptors, several modes of intermolecular interactions are conceivable. The nitro groups of DNT have been reported to bind to hydrogen bond donors and metal cations,[10,11] and there have been several publications suggesting that amines form anionic σ-complexes with DNT (often referred to as Meisenheimer complexes).[12−15] With a view to optical sensors, it appeared particularly interesting that solutions of DNT and alkylamines have a deep blue color absent to solutions of DNT or alkylamines alone.

Meisenheimer complexes have been the subject of a great deal of research[16−18] since their structure was first proposed in 1900 by Jackson and Gazzolo[19] and chemical evidence for their composition was reported by Meisenheimer in 1902.[20] These complexes result from the addition of a nucleophile to an electron-deficient aromatic molecule. Formation constants have been determined for the complexes of a wide variety of electron-deficient aromatic molecules with many nucleophiles,[6,15,21−24] and several reviews discussing recent advances made in studying such complexes were published.[16−18] Relevant to the case of DNT is that, because of their strongly electron-withdrawing nitro groups, polynitroaromatic compounds readily form Meisenheimer complexes with strong nucleophiles.[13,14,16−18,25]

The molecular structure of these complexes proved difficult to elucidate for many years, but various studies in condensed phases using UV/vis and NMR spectroscopy as well as X-ray crystallography eventually revealed that Meisenheimer complexes of polynitroaromatics consistently involve attachment of a nucleophile to an aromatic carbon in direct resonance with a nitro group.[16−18] Recently, the structure of the complex formed between 1,3,5-trinitrobenzene and methoxide has been explicitly determined in the gas phase by infrared multiphoton dissociation spectroscopy.[26] The current level of understanding indicates that strong nucleophiles result in a nearly tetrahedral geometry at the carbon center to which the nucleophile binds, while weaker nucleophiles bind in a more axial fashion with a much lesser effect on the geometry of the aromatic skeleton,[27] leading to some ambiguity as to the

Received: June 4, 2011
Published: July 07, 2011

dividing line between a Meisenheimer complex and a more weakly interacting pair.

In contrast to the extensive record on Meisenheimer complexes in general, reports on the color reaction of DNT with amines have been few. Moreover, in view of the new results described in this contribution, some of the previously reported conclusions appear to be misleading. For example, in an investigation on the formation of a colored product in solutions from DNT and butylamine, it was speculated that "dinitrotoluene, like other polynitroaromatics, is expected to form anionic sigma complexes with bases." No attempts were made to confirm the structure of these complexes.[13] Similarly, in a study of the reaction of methylamine and diethylamine with DNT in dimethyl sulfoxide (DMSO), the formation of Meisenheimer complexes was assumed only based on the analogy of similar complexes with trinitrobenzene.[14] Also, in a seminal study on the environmental fate of nitroaromatic compounds, DNT adsorption to natural clay materials with large surface concentrations of negative charges was studied. It was assumed that electron donor−acceptor (EDA) complexes were formed, but the possibility of deprotonation of DNT was not considered.[28] Arguably the most careful comment came from the developers of optical sensors based on poly(vinyl chloride) thin films doped with amines.[29] The authors did not explicitly comment on DNT complexes but stated very generally that polynitroaromatics form either Meisenheimer complexes or their conjugated bases, thus at least considering alternatives. However, as in other reports on color reactions of TNT and DNT too,[30] quantitative studies were not performed, and significant differences in the reactivities of TNT and DNT were not implied.

In this contribution, we show that DNT surprisingly does not form any appreciable amounts of Meisenheimer complexes with various alkylamines. Density functional calculations confirm the experimental conclusion that Meisenheimer complexes exist in solution as an extreme minority species at most. It is shown that the deep blue color of solutions of DNT and alkylamines in *N*,*N*-dimethylformamide (DMF) and DMSO is due to the deprotonation of DNT. The characteristic color of the deprotonated DNT was used to determine the pK_a of DNT in DMSO. The question whether hydroxide forms a complex with DNT or simply deprotonates DNT was also addressed.

2. RESULTS AND DISCUSSION

2.1. Effect of Solvent Polarity. A typical visible spectrum of a DNT−amine solution in DMSO is shown in Figure 1. Solutions of DNT with all amines studied were found to have the same broad absorbance band with a maximum at 652 nm, and in the range of 400−800 nm, all spectra overlapped with one another almost perfectly. To confirm that only one colored reaction product is formed in all solutions containing DNT and the different amines, sets of DNT−amine spectra were subjected to principle component analysis.[31] This confirmed that within experimental error only two species were responsible for the absorption in the range from 400 to 800 nm (98.7% of the spectra is described with these two components). Because DNT absorbs visible light near 400 nm, one principle component (2.2%) of the visible spectra can be attributed to DNT. The second (96.5%) principle component can then be attributed to the product of the interaction of DNT with the amine.

A large effect of solvent polarity was observed. The absorption associated with DNT deprotonation was observed in both

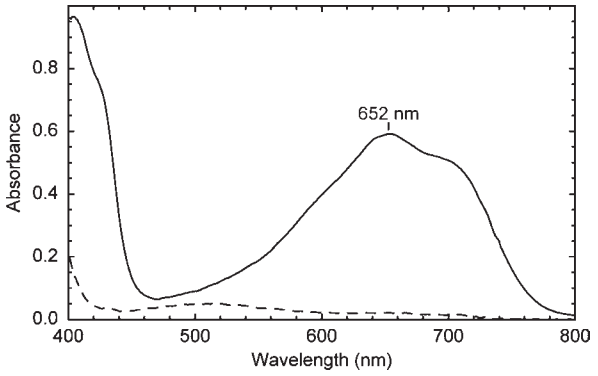

Figure 1. Visible spectrum of 10 mM DNT in DMSO before (dashed) and after (solid) the addition of 10 mM diethylamine. T = 20 °C.

DMSO and DMF but not in ethyl acetate or acetonitrile. In mixtures of either DMSO or DMF with ethyl acetate or acetonitrile, the absorption from the complex decreased sharply with the addition of even fairly small amounts (<20%) of the latter solvents. This observation is consistent with reports of Andrabi and Atehar, who reported that the formation constant of the complex of DNT with diphenylamine shows a logarithmic correlation with the π^* solvent polarity parameter of the solvent.[15] This relationship is true for complex formation in both protic and aprotic solvents. Because of the large dependence of the formation constant on the polarity of the solvent, DMSO was used for all subsequent experiments.

2.2. The Special Case of Hydroxide. The literature suggests that increased Bronsted basicity increases the stability of Meisenheimer complexes. In the case of the addition of strong nucleophiles such as methoxide to trinitrobenzene, the trinitrobenzene carbon attacked by the nucelophile was shown to take a geometry close to sp^3. In contrast, weak nucleophiles such as bromide or iodide bind to trinitrobenzene in a more axial fashion, leaving the trinitrobenzene carbon with a geometry close to sp^2.[27] Therefore, the question arose as to whether anionic species such as alkoxides or hydroxide form Meisenheimer complexes with DNT. As shown with a ^{1}H NMR titration of a DMSO-d_6 solution of DNT (100 mM) with tetrabutylammonium hydroxide, DNT behaves quite differently. Before the addition of hydroxide, DNT has aromatic protons at 7.66 (d, 1H), 8.31 (d, 1H), and 8.60 (s, 1H) ppm while the methyl peak appears at 2.63 ppm (3 H). Upon addition of a substoichiometric OH^- concentration, additional peaks were observed at 4.59 (s, 1H), 5.62 (s, 1H), 6.29 (d, 1H), 6.72 (d, 1H), and 8.56 (s, 1H) ppm, and upon addition of a full stoichiometric amount of OH^-, the original DNT peaks disappeared, leaving only the newly formed peaks. The addition of a small amount of D_2O at this point did not affect the newly formed peaks, but acidification with 5 M D_2SO_4 led to the disappearance of the OH^--induced peaks and the reappearance of the original aromatic peaks of DNT. However, the D_2SO_4 addition did not lead to the reappearance of the DNT methyl peak. This observation can be interpreted as follows: Addition of OH^- led to deprotonation of the methyl group. Because of restricted rotation around the exocyclic carbon−carbon bond, the two CH_2 protons were observed as two distinct signals at 4.59 and 5.62 ppm, while all three aromatic protons shifted upfield; these assignments are supported by density functional theory (DFT) calculations reported in Section 2.7. The addition of D_2O to the solution of the DNT anion did not

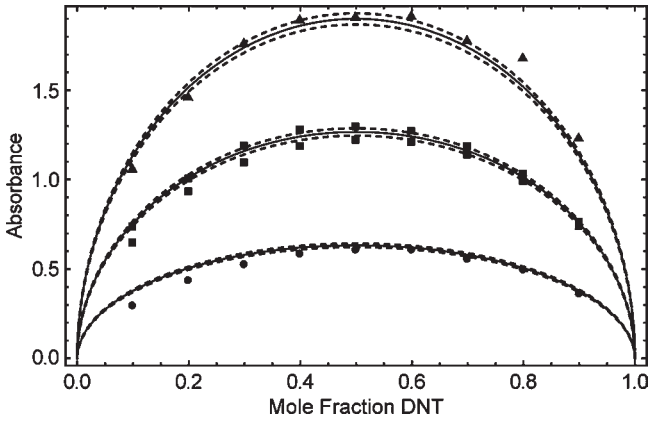

Figure 2. Job's plots and corresponding fits for the system of DNT and diethylamine (total concentration of DNT and diethylamine for the data fitted with the bottom, middle, and top curve was 20, 40, and 60 mM, respectively). The solid curves indicate the best fit while the dashed curves indicate the calculated 95% confidence intervals. $T = 22$ °C. Fitted parameter: $K_{Eq} = 2.94 \times 10^{-5}$.

result in any observable H/D exchange, but the subsequent addition of D_2SO_4 did result not only in the formation of CH_2D, but also a quickly following exchange of all methyl hydrogens to give a CD_3 group. These observations clearly show that, in DMSO, OH^- prefers to deprotonate DNT rather than produce a Meisenheimer complex by binding to DNT.

2.3. Interaction of DNT with Alkylamines. ^{1}H NMR spectroscopy also gives some insight into the interaction of DNT with amines. The ^{1}H NMR titration of 50 mM DNT with diethylamine in DMSO-d_6 showed no observable shift in the peak position or integrals of the aromatic and amine protons. Rather, the peaks corresponding to these protons only broadened very slightly, even with a large excess of the added amine. This suggests that there is a fairly quick rate of exchange between the different forms of DNT, and that, at equilibrium, either the conformations of the different DNT species are structurally very similar or that free, electrically neutral DNT remains the dominant species. As will be shown in the following, the latter is consistent with the formation of a very small concentration of deprotonated DNT.

2.4. Model for Fitting of Job's Plots. The possibility of binding of amines to DNT was further studied using Job's method of continuous variation[25,32,33] by fitting of the visible absorption at 652 nm. For each amine, several solutions were prepared to contain DNT and an amine at concentrations that added up to a constant value for all solutions of a plot. To improve the accuracy of each fit, Job's plots were prepared for several total concentrations. Job's method was initially employed because, in cases where only one complex of *n*:*m* stoichiometry is formed, it can reveal the ratio of *n* and *m* by the occurrence of a maximum in the absorbance of the complex at a host/guest ratio of *n*:*m*. However, as discussed in the following, the interpretation of a Job's plot is more complicated when the equilibrium under study involves formation of more than one product.

Experimental Job's plots for different total concentrations of DNT and benzylamine are shown in Figure 2. The three curves shown in this figure and the Job's plots for *n*-butylamine, benzylamine and triethylamine all share three characteristic features: (i) an absorption maximum was observed at a mole fraction of DNT of 0.5, indicating an equimolar stoichiometry for the reaction of DNT with the amines; (ii) none of the plots exhibited a sharp maximum, as it would be expected for the exclusive formation of a very stable complex; and (iii) all plots exhibited (with respect to the maximum absorbance at the 0.5 mol fraction of DNT) much larger absorbances around the 0.25 and 0.75 mol fraction than would be expected for the formation of one type of complex with *n*:*n* stoichiometry (such as in the case of the formation of a Meisenheimer complex). As a result, the Job's plots are more reminiscent of a semicircle than the more commonly encountered inverted parabola.[33]

The unusual semicircular shape of the Job's plots is consistent with a reactant/product ratio of 2:2 (such as for a deprotonation reaction) and a rather small equilibrium constant, while the common shape reminiscent of an inverted parabola shape is observed for a reactant/product ratio of 2:1 (such as when a host, H, and a guest, G, form HG or H_2G_2 host−guest complexes). For example, in the limit of weak complexation and 2:2 reactant/product stoichiometry, the Job's curve rises to 79% of its maximum value at a mole fraction of 0.2 (and, due to the symmetry of the curve, falls to 79% at 0.8). By contrast, the Job's curve characteristic for binding of one guest molecule to one host molecule to give a HG complex (with a 2:1 reactant/product ratio) rises for the limit of weak complexation to only 64% of its maximum at the same mole fractions. (Note that in the limit of weak complexation these percentages of maximum absorption do not depend on the actual equilibrium constant. For medium strengths of binding, the percentages become smaller for both reactant/product ratios, and for very strong binding, the Job's plots have a triangular shape.)[34]

The semicircle-type shape of the curves shown in Figure 2 strongly indicated the occurrence of a 2:2 reactant/product ratio. Indeed, various attempts to fit the experimental data with conventional models where *n* host molecules react with *n* guest molecules to form H_nG_n complexes failed because these models invariably overestimated the absorbance at the 0.5 mol fraction of DNT while simultaneously underestimating the absorbances at the 0.2 and 0.8 mol fractions of DNT. This complicated the determination of the stability of these complexes. The literature describes several fitting techniques developed to determine complex formation constants using Job's method for systems with a 2:1 reactant/product ratio.[25,35−38] However, these methods are insufficient for the determination of binding constants from experimental data in other cases. Therefore, a specific algorithm was developed in this work to fit experimental data such as those shown in Figure 2, as is described in the following.

Knowing that the reaction of DNT with an amine does not result in the simple formation of a 1:1 Meisenheimer complex or a 2:2 complex, and considering that OH^- was found to result in DNT deprotonation, the possibility of H^+ transfer from DNT to the amines was considered. This process is described by the following equations:

$$c^{\circ}_{DNT} = c_{DNT} + c_{[DNT\text{-}H]^-} \quad (1)$$

$$c^{\circ}_{A} = c_{A} + c_{AH^+} \quad (2)$$

$$K_{Eq} = \frac{c_{[DNT\text{-}H]^-} \times c_{AH^+}}{c_{DNT} \times c_{A}} \quad (3)$$

where c°_{A} and c°_{DNT} are the total amine and DNT concentrations, respectively, the *c* terms stand for the concentrations of the free species A and DNT along with the proton transfer products

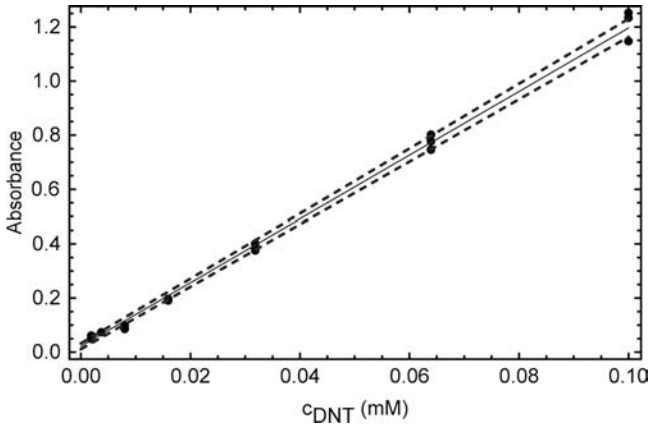

Figure 3. Absorbance of DNT in a 10 mM solution of tetrabutylammonium hydroxide in DMSO at 20 °C. The solid line represents the linear fit while the dashed curves indicate 95% confidence intervals.

$[DNT\text{-}H]^-$ and AH^+ in solution, and K_{Eq} is the equilibrium constant for the proton transfer. Since principle component analysis had shown that the system contained only one species absorbing at 652 nm, the total absorbance at this wavelength could be obtained from the concentration and molar absorptivity of the deprotonated DNT and the optical path length, d:

$$A = \varepsilon d c_{[DNT-H]^-} \quad (4)$$

Solving eqs 1−4 for the absorbance as a function of the mole ratio fraction of DNT, K_{eq}, ε, and the sum of c_A and c_{DNT} results in an equation that describes the Job's plots. This equation was used for preliminary efforts to fit the experimental Job's plots with Mathematica 7 (Wolfram Research, Champaign, IL) using an embedded nonlinear regression algorithm. However, these fits showed a poor agreement between the reported pK_a values of the amines and the fitted K_{Eq} and an extremely inconsistent molar absorptivity of the deprotonated DNT for the Job's plots with the different amines. This could be explained by that fact that, in the case of a deprotonation reaction in the limit of a small proton transfer equilibrium constant, the shape of the Job's curve when normalized to its maximum is independent of the stock concentrations, and simultaneous fitting of K_{EQ} and ε results in extremely large confidence intervals for both of these parameters.[34]

2.5. Determination of ε. To determine ε independently in a separate experiment, solutions containing 10 mM tetrabutylammonium hydroxide and DNT in a concentration range from 0.002 to 0.1 mM were prepared, and their absorbance was measured at 652 nm (see Figure 3). On the basis of the ^{1}H NMR spectra of these DNT−hydroxide solutions and the linearity of the plot in Figure 3, it was assumed that in these solutions DNT was completely deprotonated at all concentrations, and therefore, the concentration of deprotonated DNT in all solutions was equal to the total concentration of DNT. Linear regression gave the molar absorptivity of the deprotonated DNT as 11740 ± 230 M^{-1} cm^{-1}.

2.6. Determination of K_{Eq}. With the fixed value for ε, the nonlinear regression was again used to fit the Job's plots for several amines and determine numerical values for the parameters K_{Eq}. As an example, the experimental Job's plots for diethylamine at three different total concentrations along with the corresponding fits (solid lines) are shown in Figure 2. Note

Table 1. Proton Transfer Equilibrium Constants for DNT and Various Amines in DMSO at 20 °C

amine	pK_a[a]	K_{Eq}	pK_a (DNT, calculated)
benzylamine	10.2	$(4.79 \pm 0.46) \times 10^{-6}$	15.5
n-butylamine	11.1	$(9.73 \pm 0.56) \times 10^{-5}$	15.1
diethylamine	10.5	$(2.943 \pm 0.097) \times 10^{-5}$	15.0
triethylamine	9.0	$(3.75 \pm 0.47) \times 10^{-7}$	15.4
isopropylamine	Proton transfer slow. Equilibrium not achieved in 5 min.		
tert-butylamine	Proton transfer slow. Equilibrium not achieved in 5 min.		

[a] pK_a in DMSO from refs 39 and 40.

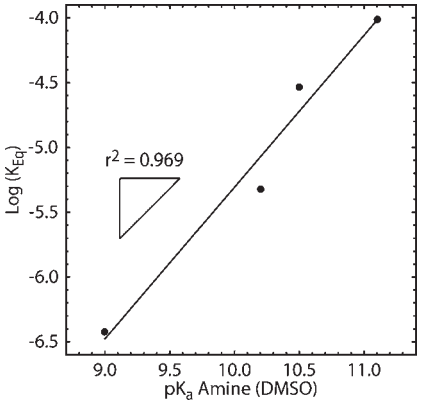

Figure 4. Log K_{Eq} vs pK_a along with the linear best fit for the amines tested in this work. The slope indicator shows the expected slope of 1.

that all 32 experimental points (i.e., all three Job's plots) were fitted simultaneously to determine one single K_{Eq} value. (The experimental Job's plots and fits for the other amine systems may be found in the Supporting Information.) The good fits of multiple Job's plots with one single value of K_{Eq} support the adequateness of our model.

The thus fitted values for the proton transfer equilibrium constants, K_{Eq}, for the different amines differ from one another by over 2 orders of magnitude (see Table 1) and reflect differences in the basicity of the amines in DMSO. This is illustrated by Figure 4, in which the logarithm of the thus determined K_{Eq} is plotted versus the pK_a of these amines in DMSO, as they were reported in the literature.[39,40] As expected, there is a linear correlation (r^2 = 0.969) between the two parameters. Moreover, the pK_a of DNT as calculated from K_{Eq} and the previously published pK_a values of the amines (15.3 ± 0.2; Table 1, right column) matches very closely the reported value for the pK_a of DNT (15.0) in a 1:1 H_2O/DMSO solution,[12] and is also consistent with DFT calculations discussed in the next section of this contribution.

As mentioned above, NMR spectra of DNT in the presence of diethylamine showed only a slight broadening of the peaks associated with the phenyl hydrogens and no significant changes in chemical shifts. In view of these fits, this can be explained easily by the extremely low values for the proton transfer equilibrium constant. At equilibrium, only 0.1% of the DNT in a 50 mM DNT/50 mM diethylamine solution is deprotonated.

It is interesting to note that, for isopropylamine and *tert*-butylamine, the deprotonation process is rather slow, presumably due to the sterically hindered accessibility of the nitrogen in these amines. While equilibrium for the other amines was achieved

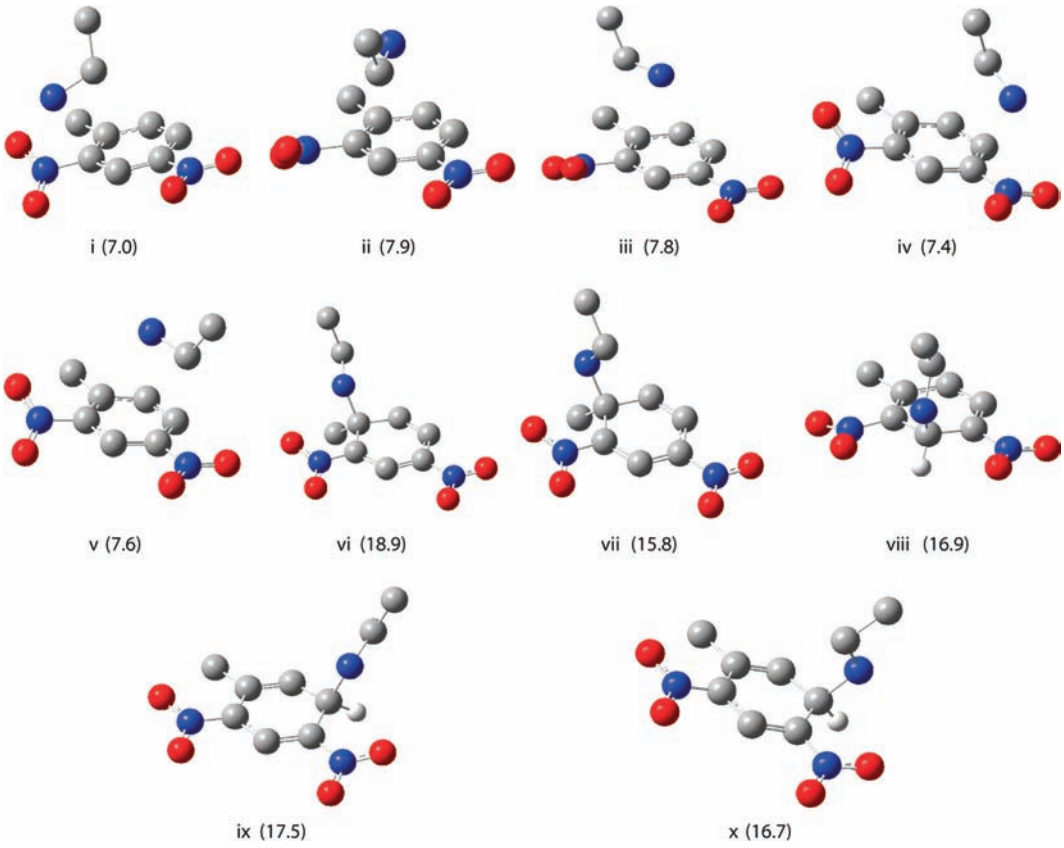

Figure 5. Optimized structures and binding free energies (kcal/mol) of 10 different complexes of ethylamine with 2,4-dinitrotoluene relative to separated components and computed at the SMD(DMSO)/M06-2X/6-311+G(2df,2p)//SMD(DMSO)/M06-2X/6-31+G(d) level including thermal contributions. Structures i−v are loose van der Waals complexes and structures vi−x are Meisenheimer complexes. Hydrogen atoms are not shown for clarity, except at the position of Meisenheimer substitution in structures viii−x; hydrogen atoms are white, carbon atoms are gray, nitrogen atoms are blue, and oxygen atoms are red.

quickly enough to allow for the determination of an equilibrium constant, deprotonation of DNT by isopropylamine and *tert*-butylamine was so slow that equilibrium was not achieved within 5 min. At these long time scales, the absorption resulting from the deprotonated DNT starts to decrease, and the solutions turn red within hours unless solutions are carefully purged with argon to remove traces of oxygen. Indeed, bubbling of oxygen into a blue solution that had kept its color for several hours after being purged with argon resulted in a color change to purple within 5 and red within 10 min. Since samples in which DNT determination is of interest always contain oxygen, further studies of the deprotonation of DNT by isopropylamine and *tert*-butylamine in an oxygen-free environment were not pursued.

2.7. Density Functional Theory Studies. To gain further insight into the surprising absence of Meisenheimer complex formation for DNT, we examined the energetics for association of DNT with ethylamine as a prototype primary amine. In particular, for various possible complex structures, we began by optimizing molecular structures at the M06-2X/6-31+G(d) level of DFT (see the Methods below for full theoretical details).

Initially, we attempted to locate Meisenheimer complexes in the gas phase by building reasonable starting geometries (with C−N bonds between appropriate aryl ring carbons and the amine nitrogen of roughly 1.45 Å) but such structures were not stable. Instead, they smoothly dissociated to van der Waals type complexes with the nitrogen lone pair clearly oriented toward some electrophilic center, but with distances only slightly less than the sum of the relevant van der Waals radii. Among the electrophilic centers were the nitrogen atoms of the nitro groups, the center of the aromatic ring, and positions axially above ring carbons at which Meisenheimer attack might be expected.

As the Meisenheimer complex of DNT and ethylamine has charge-separated character (formal resonance structures involve aci nitronates and ammonium cations), deprotonation of the NH_2 group by proton transfer to another ethylamine molecule appears plausible.[41,42] However, such a process would not result in a maximum in the Job's plot at a 1:1 mol ratio of DNT and the amine. Moreover, simple deprotonation is not possible in the case of Meisenheimer complexes of triethylamine because the nitrogen of the latter has no directly bound hydrogen. Therefore, we speculated that solvation might provide an alternative mode of stabilization of the Meisenheimer geometries. Indeed, we successfully located a number of such geometries once the effects of DMSO solvation were included in the optimization process by the use of the SMD continuum solvation model.[43] However, the loose van der Waals complexes found from the gas-phase optimizations were also determined to be legitimate equilibrium structures in DMSO solution, that is, they did not spontaneously collapse to Meisenheimer complexes. Figure 5 illustrates ten optimized structures, five of each class of complexes.

Although the Meisenheimer complexes are computed to be true equilibrium structures in DMSO solution, their free energies

are predicted to be substantially higher than those of the looser van der Waals complexes. Figure 5 lists the computed microscopic binding free energies for the various complexes, taking the convention that a positive value implies that separated species are more stable than the complex (cf. eq 5), as calculated at the SMD(DMSO)/M06-2X/6-311+G(2df,2p)//SMD(DMSO)/M06-2X/6-31+G(d) level of theory and including thermal contributions.

We emphasize the term "microscopic" when referring to complex free energies, because each binding free energy listed is for a single geometry, but it is clear that these various geometries will all be readily interconverting with one another, and presumably with many more others that we did not attempt to locate, since there are numerous different rotational possibilities associated with, for instance, the orientation of the ethyl group of the amine with respect to the ring substituents of DNT (some examples of such isomerism are included in Figure 5). In such a situation, the experimentally measured binding constant does *not* reflect the free energy of any one structure relative to separated DNT and ethylamine, but it instead reflects the relative free energy G of the entire equilibrium population of complexes, computed as[44]

$$G = -RT \ln \sum_i \exp(-G_i/RT) \quad (5)$$

where the sum runs over all conformers i, G_i is the microscopic free energy of conformer i, and R and T are the universal gas constant and temperature, respectively.

The substantial entropy associated with the very large number of possible complexes, only some of which are listed in Figure 5, will lower the population free energy significantly relative to the separated species. Moreover, it seems also likely that the first DMSO solvation shell may impart additional stability to the complexes by acting as a hydrogen bond acceptor to the amine protons that develop partial positive charge character in the bimolecular complexes. We have not attempted to model this point given the impracticality of surveying a large number of termolecular complexes at the quantum mechanical level.

We did examine the quantitative utility of the M06-2X density functional by comparing the gas-phase component of the complex interaction energies computed at the M06-2X level to values computed at the MP2/6-311+G(2df,2p) level of theory. The MP2 interaction energies were typically about 1 kcal/mol *more* favorable for the van der Waals complexes and 3 to 4 kcal/mol *less* favorable for the Meisenheimer complexes. As the density functional and correlated post-Hartree−Fock levels of theory are in reasonable agreement with one another, and as it is more difficult to achieve convergence with respect to the one particle basis set at the MP2 level,[44] we will take the M06-2X predictions to be reasonable, which is consistent with the documented strong performance of this functional in the prediction of nonbonded interactions.

Returning to the issue of the Meisenheimer complexes being substantially less stable than the looser van der Waals complexes, this observation is consistent with the NMR and UV/vis spectral data noted above. Thus, we computed ^{1}H NMR chemical shifts for DNT and complexes **i**, **v**, and **viii** following the WP06 protocol[45] with DMSO solvation. Shifting the predicted absolute shieldings so that H-6 in DNT is predicted to have its experimental chemical shift, we computed values for H-3, H-5, H-6, and the averaged methyl signal in DNT of 9.15, 8.57, 7.66, and 2.62 ppm, respectively. The relatively poor prediction of the chemical shift for H-3 compared to experiment may reflect dynamical effects associated with the nitro groups that are not taken into account in the calculations, but this point is not important for the following internal comparison. In the case of loose complexes **i** and **v**, the same proton chemical shifts are computed to be 9.07, 8.54, 7.53, and 2.61 (for **i**), and 9.15, 8.59, 7.63, and 2.62 (for **v**). The average deviation of these shifts from those for DNT itself is only 0.04 ppm. By contrast, the same proton chemical shifts predicted for the Meisenheimer complex **viii** are 6.65, 7.70, 5.41, and 2.42, respectively. Since all complexes in rapid equilibrium on the NMR time scale should contribute to the observed chemical shifts proportional to their equilibrium populations, it is clear that the amount of Meisenheimer complex(es) present at equilibrium must be *very* small in order to reconcile the experimental observation that there is no apparent change in the DNT chemical shifts upon addition of amine.

Returning to the question of the precise free energies of the Meisenheimer complexes relative to the looser van der Waals complexes, this is decidedly nontrivial to compute, although Figure 5 includes microscopic estimates. A complicating aspect is that the SMD model predicts the solvation free energies for these formally zwitterionic complexes to be from −19 to −27 kcal/mol, while for the loose van der Waals complexes values of −11 to −12 kcal/mol are computed. The potential errors are certainly on the order of 1 or 2 kcal/mol, not simply in the continuum model, but probably more importantly in the failure to account for specific DMSO solvation effects like accepting hydrogen bonds from the Meisenheimer complexes to further stabilize them.

Attempting to model more quantitatively (i) the solvent−complex interactions and (ii) the entropy associated with the phase space volume available to the many floppy complexes is well beyond the scope of this work. Nevertheless, the various computational results presented above support an interpretation of the experimental data that indicates complexes of the neutral amines and DNT (i.e., not conjugate acid/conjugate base pairs following deprotonation) to comprise a population of potentially very many loose van der Waals complexes of similar energy and also potentially many Meisenheimer complexes, but the latter are a very substantially smaller fraction of the population.

Finally, in addition to modeling Meisenheimer complexes to assess better their energetic accessibility, we also undertook DFT calculations to support our assignments of the pK_a of DNT and the ^{1}H NMR spectrum of its conjugate base. In particular, at the SMD(DMSO)/M06-2X/6-31+G(d) level of theory we computed the pK_a of DNT to be 14.5, which agrees with the measured value to within the typical uncertainty observed for computed pK_a values.[46] In addition, applying the same NMR protocol already outlined above, we predicted ^{1}H chemical shifts of 4.79 and 5.85 ppm for the exo-methylene protons of DNT conjugate base, and 6.38, 6.79, and 8.96 ppm for the aromatic protons. At this level of theory, the activation free energy for rotation of the exo-methylene (which would average its two ^{1}H signals) is predicted to be 41.5 kcal/mol, implying that no such rotation occurs on the time scale of the NMR experiment. Compared to the experimental data in Section 2.2, the predicted values have a mean unsigned error of 0.2 ppm, which is again in good agreement and consistent with assigning the conjugate base as the source of the spectrum generated upon addition of hydroxide.

3. CONCLUSIONS

We have determined that 2,4-dinitrotoluene has, despite its two nitro groups, only a small tendency to form Meisenheimer

complexes with hydroxide or basic amines in DMSO, contradicting assumptions previously made in the literature. Instead, deprotonated DNT was observed to exhibit intense absorption in the visible region, explaining the deep blue color of solutions of 2,4-dinitrotoluene and alkylamines.

Because of the wide interest in 2,4-dinitrotoluene due to environmental, toxicological, and safety concerns, the implications of our findings go beyond the development of optical sensors. The relative ease of deprotonation combined with the comparatively low tendency to interact with nucleophiles, as evidenced by our results, suggests that results from a number of recent studies on other types of 2,4-dinitrotoluene sensors may have to be critically revisited. For example, sensors based on mesoporous SiO_2,[11] TiO_2 nanowires,[10] and nanoporous silicon films as well as carbon nanotubes and graphene have been reported but the deprotonation of 2,4-dinitrotoluene on oxide surfaces or at the well-known oxygenated defects of carbon-based materials has not been considered. Similarly, electron donor−acceptor (EDA) complexes were suggested to cause adsorption of DNT to clay,[28] a more refined reinterpretation of which could have a substantial impact on our understanding of the kinetics of 2,4-dinitrotoluene transport through contaminated soils.[47] Finally, a reevaluation of the reactivity of 2,4-dinitrotoluene with special attention to deprotonation and the interaction of this nitroaromatic with nucleophiles may lead to a better understanding of the decomposition of this dinitroaromatic pollutant in the environment.

4. METHODS

4.1. Experimental Section. All reagents were used as received without further purification unless noted otherwise. Five molar D_2SO_4 (≈90 atom % D) was prepared from appropriate volumes of H_2SO_4 and D_2O. All dilute solutions for UV/vis experiments were prepared in reagent grade DMSO from Sigma-Aldrich (St. Louis, MO). 2,4-Dinitrotoluene was obtained from Alfa-Aesar (Ward Hill, MA). All amines were obtained from commercial suppliers. UV/vis absorbance spectra were obtained using a Shimadzu UV160U spectrophotometer within 5 min of preparation of the sample, unless otherwise stated in the text. All ^{1}H NMR experiments were carried out on a Varian Inova 300 MHz spectrometer.

4.2. Computational. All geometries were fully optimized at the M06-2X level[48] of density functional theory[44] making use of the 6-31+G(d) basis set.[49] The effects of DMSO solvation were included in the geometry optimizations using the SMD solvation model.[43] Thermal contributions to free energy were computed at this level of theory following the usual ideal-gas, rigid-rotator, harmonic-oscillator protocol.[44] Improved estimates of binding free energies were obtained by replacing the electronic energies computed at the M06-2X/6-31+G(d) level with single-point values computed at the M06-2X/6-311+G(2df,2p) level or at the MP2/6-311+G(2df,2p) level. ^{1}H NMR and UV/vis calculations made use of the WP06 functional/basis set combination[45] and the INDO/S model,[50] respectively. The 1 to 1 M standard-state free energy of solvation for H^+ in DMSO, required for computation of the pK_a of DNT using standard techniques,[44,46,51] was taken as −273.3 kcal/mol, as recommended by Kelly et al.[52] All calculations made use of the *Gaussian* 09 Rev A.02 suite[53] of electronic structure programs.

■ ASSOCIATED CONTENT

Ⓢ Supporting Information. Job's plots and corresponding fits for *n*-butylamine, benzylamine, and triethylamine; complete ref 51. This material is available free of charge via the Internet at http://pubs.acs.org.

■ AUTHOR INFORMATION

Corresponding Author
buhlmann@umn.edu

■ ACKNOWLEDGMENT

This work was supported by the National Science Foundation (EXP-SA 0730437 and CHE-0952054). T.T.X. thanks the ACS for Project SEED summer research I and II internships. We thank Amanda Zeise and Jing-Lei Zhang for their contribution to preliminary studies and Andreas Stein for stimulating discussions on this work.

■ REFERENCES

(1) Bond, J. A.; Rickert, D. E. *Drug Metab. Dispos.* **1981**, *9*, 10–14.
(2) Moore, D. S. *Rev. Sci. Instrum.* **2004**, *75*, 2499–2512.
(3) Steinfield, J. I.; Wormhoudt, J. *Annu. Rev. Phys. Chem.* **1998**, *49*, 203–232.
(4) Yinon, J. *Trends Anal. Chem.* **2002**, *22*, 292–300.
(5) Harper, R. J.; Almirall, J. R.; Furton, K. G. *Talanta* **2005**, *67*, 313–327.
(6) Brooke, D. N.; Crampton, M. R. *J. Chem. Soc., Perkin Trans. 2* **1982**, 231–237.
(7) Dasary, S. S. R.; Singh, A. K.; Senapati, D.; Yu, H.; Ray, P. C. *J. Am. Chem. Soc.* **2009**, *131*, 13806–13812.
(8) Karasch, C.; Popovic, M.; Qasim, M.; Bajpai, R. K. *Appl. Biochem. Biotechnol.* **2002**, *98−100*, 1173–1185.
(9) Ponnu, A.; Edwards, N. Y.; Anslyn, E. V. *New J. Chem.* **2008**, *32*, 848–855.
(10) Wang, D.; Chen, A.; Jang, S.-H.; Yip, H.-L.; Jen, A. K.-Y. *J. Mater. Chem.* **2011**, *21*, 7269–7273.
(11) Zhang, H.-X.; Cao, A.-M.; Hu, J.-S.; Wan, L.-J.; Lee, S.-T. *Anal. Chem.* **2006**, *78*, 1967–1971.
(12) Terrier, F.; Xie, H.-Q.; Farrell, P. G. *J. Org. Chem.* **1990**, *55*, 2610–2616.
(13) Qureshi, P. M.; Andrabi, S. M. A.; Saeed, A.; Ahmad, A. *Anal. Proc.* **1995**, *32*, 273–274.
(14) Hunt, A. L.; Yong, S. C. K.; Alder, J. F. *Anal. Commun.* **1996**, *33*, 323–325.
(15) Andrabi, S. M. A.; Atehar, S. *Asian J. Chem.* **2002**, *14*, 1077–1079.
(16) Artamkina, G. A.; Egorov, M. P.; Beletskaya, I. P. *Chem. Rev.* **1982**, *82*, 427–459.
(17) Strauss, M. J. *Chem. Rev.* **1970**, *70*, 667–712.
(18) Terrier, F. *Chem. Rev.* **1982**, *82*, 78–152.
(19) Jackson, C. L.; Gazzolo, F. H. *Am. Chem. J.* **1900**, *23*, 376–396.
(20) Meisenheimer, J. *Justus Liebigs Ann. Chem.* **1902**, *323*, 205–246.
(21) Crampton, M. R.; Gold, V. *J. Chem. Soc. B* **1967**, 23–28.
(22) Foster, R.; Fyfe, C. A. *Tetrahedron* **1966**, *22*, 1831–1842.
(23) Fyfe, C. A. *Can. J. Chem.* **1968**, *46*, 3047–3054.
(24) Ryzhova, G. L.; Rubtsova, T. A.; Vasil'eva, N. A. *Zh. Obshch. Khim.* **1966**, *36*, 2031–2035.
(25) Schaeppi, Y.; Treadwell, W. D. *Helv. Chim. Acta* **1948**, *31*, 577–588.
(26) Chiavarino, B.; Crestoni, M. E.; Fornarini, S.; Lanucara, F.; Lemaire, J.; Maitre, P. *Angew. Chem.* **2007**, *46*, 1995–1998.
(27) Chiavarino, B.; Crestoni, M. E.; Fornarini, S.; Lanucara, F.; Lemaire, J.; Maitre, P.; Scuderi, D. *Chem.—Eur. J.* **2009**, *15*, 8185–8195.
(28) Haderlein, S. B.; Weissmahr, K. W.; Schwarzenbach, R. P. *Environ. Sci. Technol.* **1996**, *30*, 612–622.
(29) Gheorghiu, L.; Seitz, W. R.; Arbuthnot, D.; Elkind, J. L. *Proc. SPIE* **1999**, *3853*, 296–302.
(30) Jenkins, T., F.; Walsh, M. E. *Talanta* **1992**, *39*, 419–428.

(31) Otto, M. *Chemometrics: Statistics and Computer Application in Analytical Chemistry*; Wiley-VCH: New York, 1999.
(32) Job, P. *Ann. Chim.* **1928**, *9*, 113–203.
(33) Connors, K. A. *Binding Constants: The Measurement of Molecular Complex Stability*; John Wiley & Sons: New York, 1987.
(34) Olson, E. J.; Bühlmann, P., in preparation.
(35) Likussar, W.; Boltz, D. F. *Anal. Chem.* **1971**, *43*, 1265–1272.
(36) Betts, R. H.; Michels, R. K. *J. Chem. Soc.* **1949**, S286–S294.
(37) Likussar, W. *Anal. Chem.* **1973**, *45*, 1926–1931.
(38) Vosburgh, W. C.; Cooper, G. R. *J. Am. Chem. Soc.* **1941**, *63*, 437–442.
(39) Kolthoff, I. M.; Chantooni, M. K.; Bhomik, S. *J. Am. Chem. Soc.* **1968**, *90*, 23–28.
(40) Crampton, M. R.; Robotham, I. A. *J. Chem. Res., Synop.* **1997**, 22–23.
(41) Bernasconi, C. F. *Acc. Chem. Res.* **1978**, *11*, 147–152.
(42) Bernasconi, C. F.; Muller, M. C.; Schmid, P. *J. Org. Chem.* **1979**, *44*, 3189–3196.
(43) Marenich, A. V.; Cramer, C. J.; Truhlar, D. G. *J. Phys. Chem. B* **2009**, *113*, 6378–6396.
(44) Cramer, C. J. *Essentials of Computational Chemistry: Theories and Models*, 2nd ed.; John Wiley & Sons: Chinchester, 2004.
(45) Wiitala, K. W.; Hoye, T. R.; Cramer, C. J. *J. Chem. Theor. Comput.* **2006**, *2*, 1085–1092.
(46) Ho, J. M.; Coote, M. L. *Theor. Chem. Acc.* **2010**, *125*, 3–21.
(47) Uchimiya, M. *Aquat. Geochem.* **2010**, *16*, 547–562.
(48) Zhao, Y.; Truhlar, D. G. *Theor. Chem. Acc.* **2008**, *120*, 215–241.
(49) Hehre, W. J.; Radom, L.; Schleyer, P. V. R.; Pople, J. A. *Ab Initio Molecular Orbital Theory*; Wiley: New York, 1986.
(50) Zerner, M. C. *Rev. Comp. Chem.* **1991**, *2*, 313–365.
(51) Kelly, C. P.; Cramer, C. J.; Truhlar, D. G. *J. Phys. Chem. A* **2006**, *110*, 2493–2499.
(52) Kelly, C. P.; Cramer, C. J.; Truhlar, D. G. *J. Phys. Chem. B* **2007**, *111*, 408–422.
(53) Frisch, M. J.; et al. ; *Gaussian 09*, Rev A.02; Gaussian, Inc.: Wallingford, CT, 2010.